

Geothermal Prospect Zone Estimation Based on Landsat 8 Satellite Imagery (Case Study Around Gedongsongo)

Alma Izzatinavia¹, Tony Yulianto¹, M. Irham Nurwidyanto¹

¹Department of Physics, Faculty of Science and Mathematics, Diponegoro University, Semarang Indonesia.

Corresponding Author: Tony Yulianto

DOI: <https://doi.org/10.52403/ijrr.20240609>

ABSTRACT

Indonesia possesses significant geothermal potential due to its geographical location situated among three active tectonic plates. The vast geothermal potential has led to a portion of it being underexploited due to the difficulty in identifying the exact locations field of geothermal potential. Hence, exploration activities are required to discover these potential geothermal sites without direct field explorations. The geothermal potential that needs further development lies in the Gedongsongo area, District, Semarang, Central Java, specifically on the southern slopes of Mount Ungaran. This research aims to map the surface temperature and estimate geothermal potential areas in the study area using Landsat 8 satellite image data. The analysis of surface temperature mapping can utilize remote sensing by leveraging thermal images from satellite data using the Normalized Difference Vegetation Index (NDVI) method, Land Surface Temperature (LST) method, and Fault Fracture Density (FFD) method. The overlay results of these three parameters produced a geothermal potential map in the areas of Candi Village and Kenteng Village, indicating several areas predicting geothermal potential. In Candi Village, three potential geothermal areas were identified with high and very high potential levels, having a moderate lineament density ranging from 1.07 to 1.8 km², with ground surface

temperatures ranging from 21 to 26 °C. For the potential areas in Kenteng Village, two potential geothermal areas were found with high and very high potential levels, showing a density of 1.8 to 5.78 km², and ground surface temperatures ranging from 21 to 26 °C.

Keywords: *Gedongsongo, remote sensing, vegetation density, land surface temperature, fracture density*

INTRODUCTION

Indonesia has great geothermal potential because of its geographic location between three active tectonic plates, namely the Eurasian plate, the Indo-Australian plate and the Pacific plate. The impact of the meeting of these three plates makes Indonesia one of the regions with high geological activity in the world [1]. Part of this potential comes from the ring of fire that crosses Indonesia, which is one of the potential geothermal sources. Geothermal energy itself is heat energy produced from within the earth. Indonesia has geothermal potential reaching 40% of the total geothermal energy in the world, or around 29,000 MW and Indonesia is a country with very high volcanic potential [2].

Based on data from the Geological Agency, only 8.9% or 2,130.6 MW of geothermal potential in Indonesia has been utilized and there is still a lot of geothermal potential that has not been utilized [3]. This is because

exploration activities to find geothermal potential locations are very difficult to carry out in the field. Apart from that, equipment costs are expensive and exploration activities take a long time, so to optimize the development and utilization of geothermal energy, exploration activities are needed to find geothermal potential location points without carrying out exploration activities directly in the field.

This geothermal manifestation has appeared in various places, one of which is in Gedongsongo in the Mount Ungaran area. Gedongsongo Temple has geothermal manifestations such as fumaroles, hot springs, hot soil and altered rocks [4]. Mount Ungaran was formed as a result of volcanic tectonic movements in the northern part of the North Serayu Mountains and has a height of 2,050 meters above sea level. This area needs to be developed further because it is a geothermal prospect area with geothermal potential of 50 Mwe [5].

Geothermal exploration activities that are easy to carry out without having to come directly to the research area are by using remote sensing applications. Remote sensing methods simplify exploration problems such as time efficiency, economy and ease of exploration locations. Remote sensing can have the ability to provide important information about various things, including vegetation, lithology, geological orientation, and changes in heat sources based on energy absorption by rocks and the composition of the earth's surface [6].

Remote sensing satellite data can be used to identify land surface temperature, namely by using Landsat 8 imagery. The data used for the process of identifying land surface temperature as a geothermal prospect zone uses Landsat 8 satellite imagery, namely vegetation density, land surface temperature and lineament density. To identify LST, the digital value is converted into a radian value, then the radian value is converted into temperature units which can provide more specific information about land surface temperature.

For this reason, satellite image data processing can be used as initial data for geothermal exploration by displaying the condition of the earth's surface in various types of views, conditions and scales. Landsat satellite imagery can be used to map and display geological, lithological and land structures on the surface [7]. Therefore, this research was conducted to map land surface temperatures to determine the existence of geothermal prospect zones around Gedongsongo which were measured using Landsat 8 imagery. This research can help identify large areas, at affordable costs, and requires a relatively short time to develop geothermal resources.

LITERATURE REVIEW

Remote Sensing

Remote sensing refers to scientific methods and scientific analysis techniques that allow users to obtain data information about objects on the earth's surface without having direct interaction with the object being observed [8].

The remote sensing system mechanism begins by recording the appearance of the earth's surface by analyzing electromagnetic radiation. When an object emits energy, the sensor will collect and record electromagnetic radiation at a long distance without touching the object. The sensor will record, then the information will be sent and processed into digital image data [9].

Landsat 8 image

Landsat or better known as *land satellite* is an example of the first remote sensing satellite launched by NASA in the United States in 1972 with the name ERTS-1 (*Earth Resources Technology Satellite-1*). Landsat is divided into two, namely the first generation (experimental) which includes Landsat 1-3 and the second generation (operational) which includes Landsat 4-8 [10].

Landsat 8 has the ability to record images at various spatial resolutions. Landsat 8 uses two passive sensors, namely: OLI and TIRS [11]. Landsat 8 with 11 bands makes it

capable of collecting 400 image scenes in one day of recording. This makes Landsat 8 have 150 times more than Landsat 7 which only has 7 bands [12]. When analyzing Landsat image data, each band must be combined to obtain an image representation that meets the analysis objectives.

Normalized Difference Vegetation Index (NDVI)

Vegetation density is a parameter that is widely used to visualize the level of health, vegetation density and greenness. Vegetation density is a value that can be calculated by comparing the brightness of band 4 (*red band*) and band 5 (*near infrared band*). The NDVI value is determined using the following equation [2].

$$NDVI = \frac{(NIR-RED)}{(NIR+RED)} \quad (1)$$

where, the *RED* value is *red bands* 4 and *NIR* is *near infrared band* 5. Vegetation density has an NDVI value range of -1 to 1, a value of -1 indicates a classification of very low density and an NDVI value of 1 indicates it is classified as a high level of vegetation density.

Land Surface Temperature (LST)

Land surface temperature is a condition that is controlled by the balance of energy, thermal properties, and atmospheric conditions at the surface [13]. Surface temperature calculations utilize radiation temperature value data obtained from satellite reflectance at band 10 and band 11 from the TIRS sensor for Landsat 8 imagery. To convert digital values from band 10 into spectral radiance (L_λ), the equation used is as follows: [14].

$$L_\lambda = (M_L \times) + A_L \quad (2)$$

in the equation, L_λ represents reflectance, while M_L namely radiance or reflectance multiplicative band x , where x is the band number, A_L namely radiance or reflectance add band x , where x is the band number, Q_{cal}

namely the digital number value. Then the *reflectance* value is converted to the *Brightness Temperature equation*. Calculation of the *Brightness Temperature value* uses the following equation [15].

$$BT = \frac{K_2}{\ln\left(\frac{K_1}{L_\lambda} + 1\right)} - 273 \quad (3)$$

where, BT is *brightness temperature* (K), L_λ namely *To A spectral radiance* ($Watt/m^2 srad \mu m$), K_1, K_2 that is conversion constant in the thermal band.

The average emissivity of the earth's surface is calculated based on the NDVI value. After that, the vegetation fraction or PV value can be calculated using the following equation [16].

$$PV = \left[\frac{(NDVI-NDVI_{min})}{(NDVI_{maks}+NDVI_{min})} \right]^2 \quad (4)$$

where, PV is the value of *proportion of vegetation*, $NDVI$ is the NDVI value at each *pixel*, $NDVI_{min}$ namely minimum NDVI value, $NDVI_{maks}$ is maximum NDVI value. The NDVI value is very responsive to vegetation conditions, therefore, identifying these conditions can be estimated using equation 2.4, expressed as follows [17].

$$LSE = m \times PV + n \quad (5)$$

where, LSE is *Land Surface Emissivity*, PV is *proportion of vegetation*, m is a constant value of the standard deviation of surface emissivity (0.004), where n the vegetation emissivity value is reduced $m(0.986)$. Then, find the *Land Surface Temperature* (LST) value using the following equation [16].

$$LST = \frac{BT}{\left[1 + \left(\frac{\lambda(BT)}{\rho}\right) \ln LSE\right]} \quad (6)$$

Where, LST is *Land Surface Temperature* ($^{\circ}C$), is ρ Planck's constant ($1.438 \times 10^{-2} mK$), BT is *Brightness temperature* (K), LSE is *Land Surface Emission*, and λ is the

wavelength of radiation emitted in the radian band (μm).

Geological Lineaments

Straightness or *Lineament* is the proximity of a surface line pattern that can be distinguished and mapped and reflects subsurface conditions [18]. The morphological impression on the lineaments visible on the earth's surface is caused by the influence of geographic forces from within the earth. The morphological expression recorded by images is an orientation in remote sensing [19].

One way to identify geological structures is to carry out lineament density analysis.

Lineament maps provide information on fault and fracture density anomalies. The greater the level of density of the structure, the greater the level of permeability. Therefore, areas with high lineament density anomalies have the best permeability [20].

MATERIALS & METHODS

This research took the study area of Candi Village, Bandungan District, Semarang, Central Java, which has geothermal manifestations, namely hot springs and fumaroles. The data sources used are Landsat 8 data which can be accessed on the USGS (*United State Geological Survey*) website, and DEMNAS data on the BIG website. The research location can be seen in **Figure 1**.

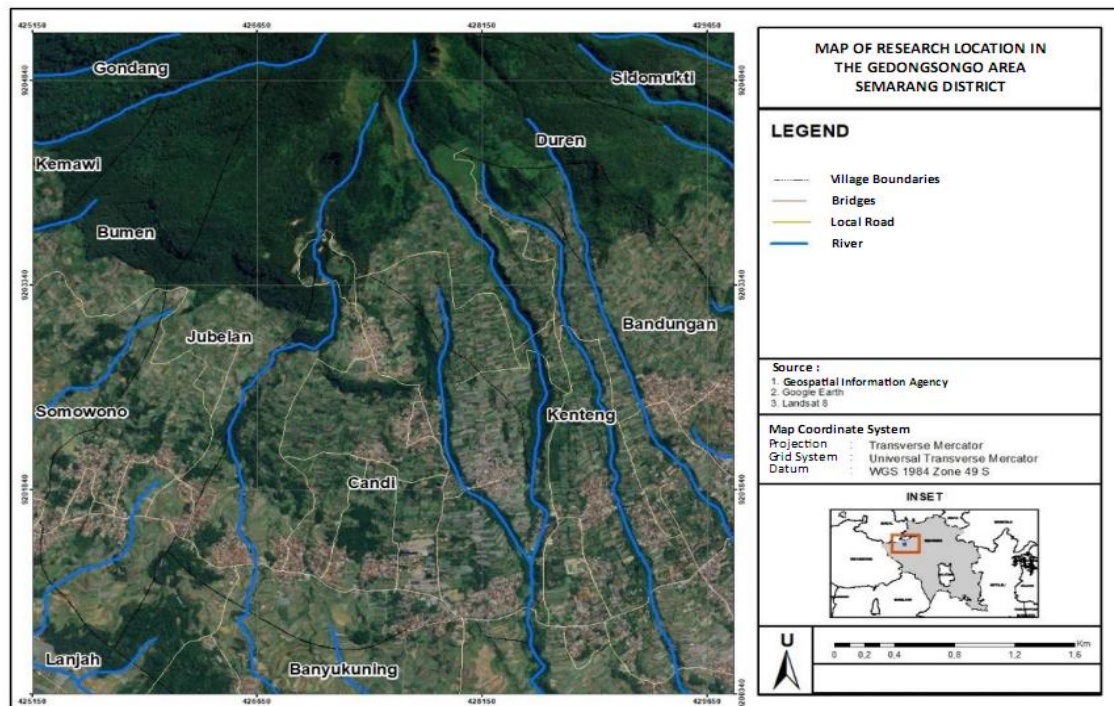


Figure 1. Map of Research Area

1. Stages of Research Implementation

Some of the steps used in this research include:

a. Study of literature

The process of searching for reference information and reviewing theories related to the research subject to be carried out. The aim of this literature study is to obtain information to strengthen the problem being studied and provide a theoretical basis for further research.

b. Data collection

Downloading Landsat-8 imagery is done via the official USGS website. The downloaded image is selected based on *path/row* recording time, and image brightness quality that is appropriate to the research area. Download DEM data via the official BIG website.

c. Data Pre-Processing

The data pre-processing stage is carried out by radiometric correction of satellite image data and image cropping.

i. Radiometric Correction

Radiometric correction functions to eliminate radiometric errors in the image and improve the overall quality of the image. Additionally, radiometric correction is also useful in multitemporal and multisensor data analysis for interpretation as well as continuous change detection [21]. In image processing, radiometric correction converts data from digital number (DN) format to radians, then convert it into a reflectance value, except for the thermal band which is converted into a brightness temperature value (BT) [22].

ii. Image Cropping

Image cropping is done to obtain an image that only covers the research area. The goal is to reduce the time and resources required to carry out the analysis process. Image cutting process with reference to the administrative boundaries of Semarang Regency taken from the RBI map in Shp (*shapefile*) format with a scale of 1:25,000. Image cropping can be done using image processing software.

d. Data processing

The data processing stages are carried out after obtaining all the necessary data. The research data that has been downloaded is then processed using ArcGis software to determine ground surface temperature and lineament density.

i. Land Surface Temperature

The purpose of this data processing process is to extract LST (*Land Surface Temperature*) values in the research area.

ii. TOA Radiance Value

Radiance value is important in satellite image analysis because it can be used to calculate various parameters, one of which is land surface temperature.

iii. Brightness Temperature Value

Brightness *Temperature* used to measure the temperature of objects or the earth's surface at the time satellite images are recorded, which is called potential temperature.

However, this potential temperature is not always the same as the actual temperature when the measurement is taken, because the temperature can change over time and depends on various factors such as the time of shooting, weather conditions, and so on.

iv. Normalized Difference Vegetation Index value

The NDVI algorithm is used to obtain vegetation density values in an area. This is done by comparing the near infrared reflectance (NIR) value from *band 5* and the red reflectance (Red) from *band 4* in satellite images, where areas with healthy vegetation have higher NDVI values.

v. Emissivity Value

The nature of the material, surface texture, surface condition, temperature, and other factors greatly influence the emissivity value of an object. In analyzing the earth's surface temperature using remote sensing data, emissivity is an important component in converting the thermal radiation value received by the sensor into temperature.

vi. Land Surface Temperature (LST) Value

The LST value is obtained if the *Brightness Temperature value* and emissivity value have been obtained. After the LST value is known, continue to create a land surface temperature map based on the LST value obtained from the extraction process from previous image processing.

2. Lineament Density Data Processing

Data processing uses DEMNAS data to obtain lineament extraction using *software Global Mapper 23* and ArcGIS 10.8. The *fault fracture density (FFD)* method is used to determine geothermal areas based on lineament density. Lineaments here are considered as weak planes associated with faults and cracks in *reservoirs* that appear on the surface in the form of manifestations such as fumaroles or hot springs. The analysis results are in the form of a lineament density map.

This method produces lineaments that are related to the structure and reflection of topographic features such as the straightness of rivers, valleys, faults and fractures, as well as the emergence of geothermal

manifestations [23].

The parameters of lineament density, land surface temperature, and vegetation density are overlaid to map the geothermal heat of

the Gedongsongo area. This is done using scoring and weighting which can be shown in **Table 1**.

Table 1. Scores and Weighting [24]

Parameter	Classification	Score	Weight
Normalized Dence Vegetation Index (NDVI)	No Vegetation	5	20%
	Very Low Density Vegetation	4	
	Low Density Vegetation	3	
	Moderately Density Vegetation	2	
	Highly Density Vegetation	1	
Land Surface Temperature	9-14 °C	1	40%
	14-17 °C	2	
	17-19 °C	3	
	19-21 °C	4	
	21-26 °C	5	
Dense of Lineament	Very Low	1	40%
	Low	2	
	Moderate	3	
	High	4	
	Very High	5	

1. Data analysis method

Data analysis was obtained from the results of data processing consisting of land surface temperature maps, vegetation density maps, and lineament density maps. This data analysis was carried out to identify vegetation density maps, land surface temperature maps, and lineament density maps through an image interpretation process to see color changes. The results of *overlaying* vegetation density maps, land surface temperature maps, and lineament density maps, were then analyzed and mapped to obtain information on the level of geothermal potential in the research area. Furthermore, information about the level of geothermal potential in the research area is

presented in the form of reports and maps that explain in detail the results of the analysis.

RESULT AND DISCUSSION

1. Analysis Normalized Difference Vegetation Index (NDVI)

Based on the density of vegetation in the research area shown by the NDVI map (**Figure 2**), the maximum NDVI value was obtained, namely 0.61 and the minimum NDVI value was -0.0003. NDVI value is positive (+) indicating the area has vegetation, while the NDVI value is negative (-) indicating the research area has surface water or clouds [25].

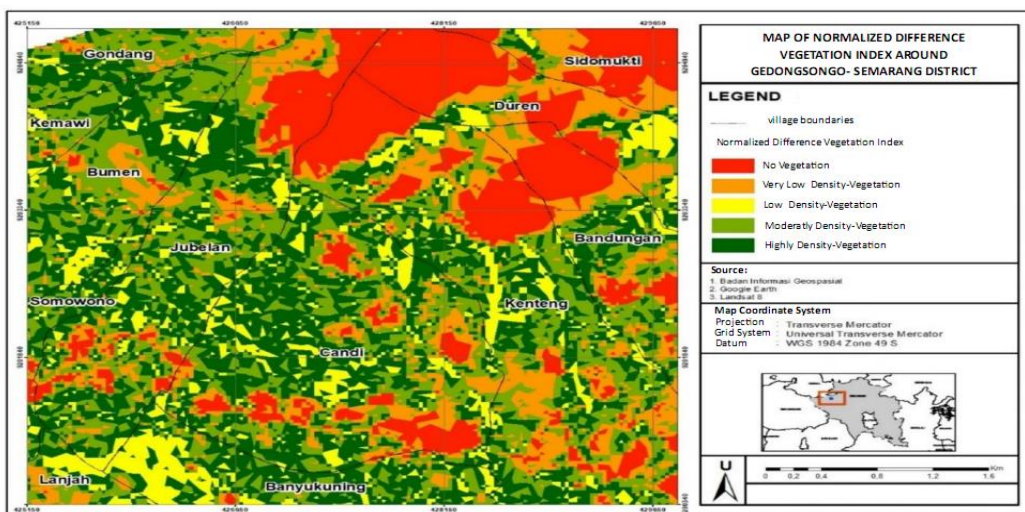


Figure 2. Vegetation Density Map

The results of NDVI image processing produce information about the density distribution. In the processing results, various different color classifications are shown based on the level of vegetation in the study area. These colors are caused by reflectance from vegetation imaging in the study area. Areas with high vegetation density usually have low surface temperatures, and vice versa. This is assumed to be because the tendency for temperatures to decrease is influenced by low vegetation density. Vegetation density can be indicated as one of the potential factors for geothermal manifestations below the surface. Vegetation with high density has lower geothermal potential than vegetation with low density [26].

2. Analysis Land Surface Temperature (LST)

Land Surface Temperature (LST) is the average surface temperature of an object as an initial exploration to identify any anomalies in the research area, where high land surface temperatures can be used as a reference in detecting geothermal potential to determine the existence of geothermal

potential. because land surface temperature is related to subsurface geothermal sources.

Surface temperatures in the study area range from 9°C to 26°C and in the Gedongsongo hot springs area the surface temperature is 14°C to 17°C. In **Figure 3** LST map, various different color classifications are shown based on surface temperature levels in the study area.

According to the results of Landsat 8 image data processing, it can be seen that the distribution of land surface temperatures in most of the study area ranges from 19°C to 21°C, with low temperatures of 9°C to 17°C thought to be caused by cloud cover. The highest temperature found at several points in the study area was 21°C to 26°C, it is estimated that this area is a residential area or an area related to geothermal system activity. Ground surface temperature is higher in an area, then in that area it is suspected that there is a geothermal anomaly [27]. Subsurface geothermal manifestations can indicate the presence of geothermal anomalies that can affect the surface temperature of the land in the area. With geothermal manifestations in the research area, a review can be carried out to determine geothermal potential.

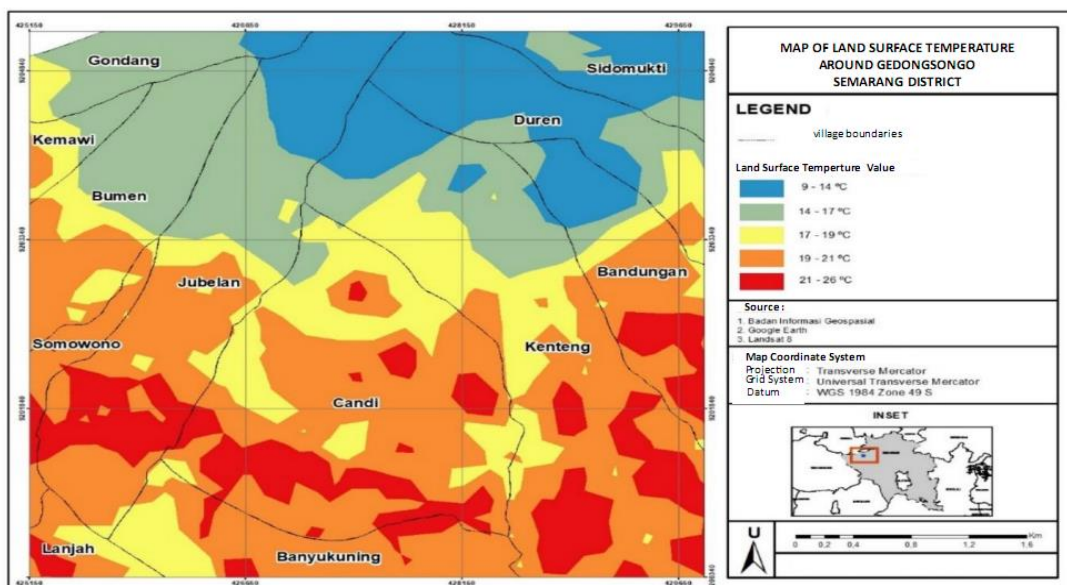


Figure 3. Land Surface Temperature Map

3. Lineament Density Analysis

Lineaments are formed as a result of geological processes recorded by remote

sensing images. The results of DEMNAS data processing determine the lineament density which correlates the density level of

geological structures with the density and permeability levels of the research area. After interpretation, a lineament density map or FFD was created which is shown in **Figure 4**. The research results show the lowest value is 0 - 0.4 km/km² and the highest value is 2.96 - 5.78 km/km². High lineament density values are distributed in the east and west, while low lineament density values are distributed in the northwest and southeast. A high lineament density value indicates that the area has good permeability.

Straightness is a surface topographic characteristic that indicates the presence of weak zones [28]. Map straightness density shown in **Figure 4**. The trend of lineament orientation in this area has a northeast – southwest orientation. Straightness controls the density level in the research area. The tighter the alignment, the better density value is also greater, which means the permeability level of the area is also greater. To determine the weakest zone as a geothermal manifestation, lineament density mapping is used to indicate the permeable zone in the research area [29].

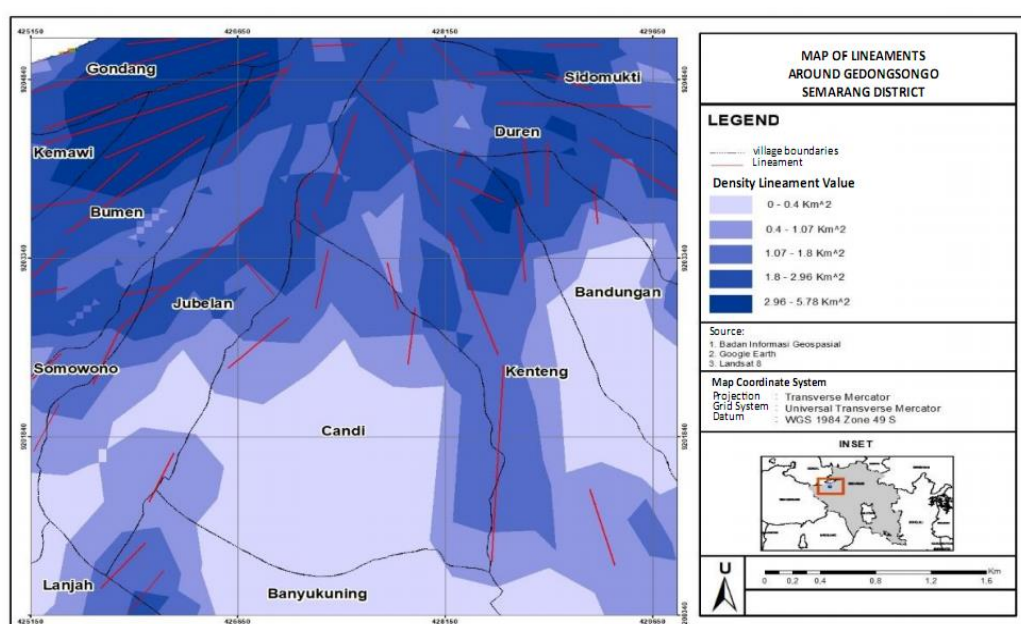


Figure 4. Lineament Density Map

5. Geothermal Potential Mapping

This research carried out geothermal mapping using Landsat 8 image data in the Gedongsongo area. Gedongsongo's geothermal potential can be exploited further because it is located on the slopes of Mount Ungaran, where manifestations in the form of fumaroles, hot springs and alteration rocks are often found around the Gedongsongo area.

Geothermal manifestations occur on the ground surface as indicated by signs of

geothermal activity below the surface. Geothermal detection mapping is obtained from the overlay of NDVI, LST and lineament density parameters for initial detection of geothermal presence in the research area using scoring and weighting techniques [26].

Determining geothermal potential areas uses parameters such as density, permeability, LST value, NDVI value and the presence of manifestations. NDVI values have a good correlation with LST values.

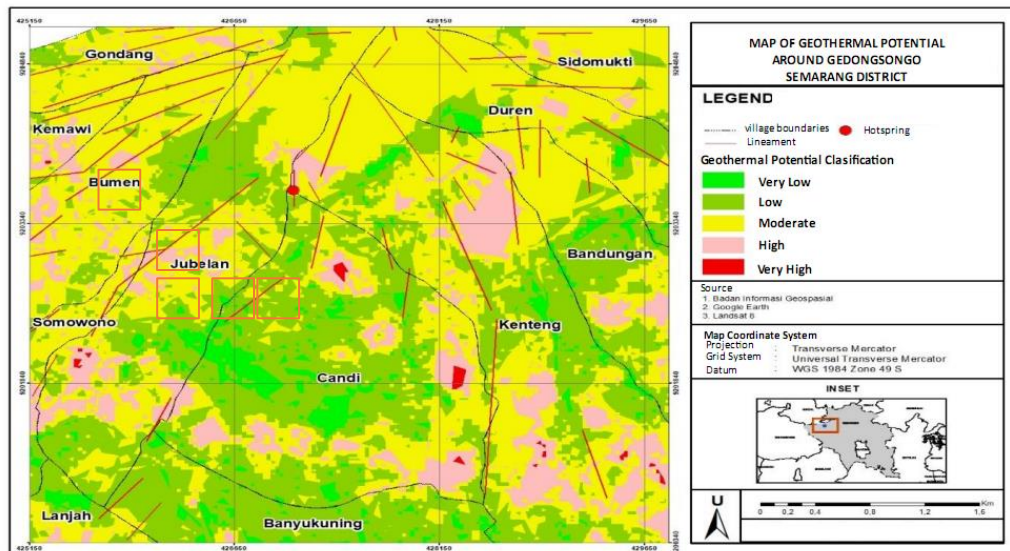


Figure 5. Geothermal Potential Map

In **Figure 5**, the area with hot springs is located at the top of Candi Village, where this area has a high level of geothermal potential. The vegetation density in this area is included in the non-vegetation density with a ground surface temperature ranging from 14 - 17 °C, which indicates that the area has a low ground surface temperature classification. This happens because the density of vegetation in the area can be in the form of water, residential areas, open empty land or areas with damaged vegetation conditions. This area also has a high lineament density, which ranges from 1.8 – 2.96 per km², which indicates that in this area there is good permeability because the lineaments control the density level in the study area, so the tighter the straightness, then the density value is also greater, which means the permeability level of the area is also greater.

Based on the map analysis carried out in **Figure 5**, there are similarities between geothermal potential areas and the potential results from Saraswati's research in 2019[30]. In this research, geothermal potential areas were found in Gedongsongo, namely in Kenteng Village and Candi Village. Based on the geothermal potential areas which can be seen in **Figure 5**, the Candi Village and Kenteng Village areas have several areas that have high and very high levels of potential.

There is an estimate of the geothermal potential area in Candi Village which has three geothermal potential areas with high and very high potential levels which have a moderate lineament density value of 1.07 – 1.8 km², with a ground surface temperature of 21-26 °C. For the potential area in Kenteng Village, there are two geothermal potential areas with high and very high potential levels which have a density value of 1.8-5.78 km², with a ground surface temperature of 21-26 °C. According to research by Saraswati (2019)[30], an energy calculation of 81,604 MW was obtained, where this value will later be subtracted from the total estimated geothermal energy from potential areas with non-potential areas so that the energy yield obtained in Candi Village and Kenteng Village is 25,059 MW.

CONCLUSION

1. Mapping of land surface temperatures in the area around Gedongsongo is spread across most of the study area, ranging from 19°C to 21°C, with low temperatures of 9°C to 17°C thought to be caused by cloud cover. The highest temperature found at several points in the study area was 21°C to 26°C, it is estimated that this area is a residential area or an area related to geothermal system activity.
2. The results of the geothermal potential map based on vegetation density, ground

surface temperature, and lineament density showed that the geothermal potential area map is found in the Candi Village and Kenteng Village areas which have several geothermal potential estimation areas in Candi Village which has three geothermal potential area points. with a high and very high potential level which has a medium lineament density value of 1.07-1.8 km², with a ground surface temperature of 21-26 °C. For the potential area in Kenteng Village, there are two geothermal potential areas with high and very high potential levels which have a density value of 1.8-5.78 km², with a ground surface temperature of 21-26 °C

Declaration by Authors

Acknowledgement: None

Source of Funding: None

Conflict of Interest: The authors declare no conflict of interest.

REFERENCES

1. Manyoe, IN, Irfan, UR, and Suriamiharja, DA 2015. Distribution of Magnetic Anomalies in the Bongongoayu Geothermal Area, Gorontalo. National Scientific Seminar on Strengthening Partnerships Based on Science and Technology Innovation for the Benefit of BMI. Faculty of Engineering, Hasanuddin University Makassar. Indonesia.
2. Wahyuni, N. 2012. Indonesia will become the largest producer of geothermal electricity in the world.
3. Directorate General of EBTKE. 2020. Huge Untapped Potential, 46 Geothermal Projects Ready to Run. Accessed December 26, 2023, from <https://ebtke.esdm.go.id>
4. Zarkasyi, A., Yuanno A and Mochamad N. 2011. Geothermal Prospects for Mount Ungaran Based on Integrated Geoscience Analysis. Geological Resources Bulletin 6(3): 23-29.
5. Tarmidhi. 2013. Study of Fluid Flow in the Geothermal Manifestations of Gedongsongo Temple Based on Geophysical Data. Semarang: Diponegoro University.
6. Frutuoso, RMDC (2015). Mapping Hydrothermal Gold Mineralization Using Landsat 8 Data. A case of study in Chave license, Portugal: Dissertação deMestrado.
7. Azmi, EA U and Danoedoro, P. 2016. Landsat 5 and SRTM analysis to identify geological structures as a first step in determining the location of geothermal potential for hydrocarbon deposits in parts of the Pantura of Central Java. Indonesian Earth Journal, 5.3.
8. Lillesand, TM and Kiefer, RW 1979. Remote Sensing and Image Interpretation . Yogyakarta: Gadjah Mada Press.
9. Aggarwal, S. 2009. Principles of Remote Sensing. Satellite Remote Sensing and GIS Application in Agricultural Meteorology. Indian Institute of Remote Sensing: Dehra Dun. 23-38.
10. USGS. 2018. Landsat Mission . <https://eros.usgs.gov/>.
11. USGS. 2013. Landsat Processing Details. http://landsat.usgs.gov/Landsat_Processing_Details_php
12. Lillesand TM and Kiefer, RW 1990. Remote Sensing and Image Interpretation. 3rd edition . New York: John Wiley and Sons, Inc.
13. Riyadhi, AF, Wardhana, FS, and GNR, PJ (2017). Analysis of Land Surface Temperature Distribution in Tompasso, Minahasam, North Sulawesi Using Landsat-8 Satellite Imagery. 10th National Earth Seminar (pp. 1827-1835). Yogyakarta: Faculty of Engineering UGM.
14. USGS. 2015. LSDS Version 1.0: LANDSAT 8 (L8) Data Users Handbook. Department of the Interior US Geological Survey, Sioux Falls, South Dakota.
15. Ibrahim, F., Atriani, F., Wulan, R., Putra, MD, and Maulana, E. (2016). Comparison of Landsat 8 Tirs Brightness Temperature Extraction Without Atmosphere Correction. Proceedings of the UMS National Geography Seminar.
16. Sobrino, J.A., J.C. Jeminez-Munoz. and Polini, L. 2004. Land Surface Temperature Retrieval from Landsat TM 5. Remote Sensing of Environment. 90. 434-440.
17. Rajeshwari, A., and Mani, ND 2014. Estimation of Land Surface Temperature of Dindigul District Using Landsat 8 Data. International Journal of Research in Engineering and Technology (IJRET), Vol. 3, Issue 5, 122-126.
18. O'Leary, D.W., Friedman, J.D., and Phn, H.A., (1976). Lineament, Linear, Lineation: Some proposed new standard for old terms. Geol. Soc. Amer. Bull., Vol. 87 pp. 1463-1469.

19. Abdullah F. A., Lalit Kumar, L., 2013. Investigating the Use of Remote Sensing and GIS Techniques to Detect Land Use and Land Cover Change: A Review. *Advances in Remote Sensing*, 2013, 2, 193-204.
20. Pambudi, N.A., Itoi, R., Jalilinasraby, S., Jaelani, K., 2014. Exergy Analysis and Optimization of Dieng Single-Flash Geothermal Power Plant. *Energy Conversion and Management*, Volume 78, pp. 405–411
21. Kustiyo, Dewanti, R., and Lolitasari, I. 2014. Development of a Multi-Spectral and Multi-Temporal SPOT 4 Image Radiometric Correction Method for Image Mosaics. *National Seminar on Remote Sensing 2014* (p. 80). Jakarta: Center for Remote Sensing Technology and Data, LAPAN.
22. Congedo, L. 2016. Semi-Automatic Classification Plugin Documentation . DOI: <http://dx.doi.org/10.13140/RG.2.2.29474.02242/1>
23. Yanis, M., Ismail, N., Hermansyah, L.V., Nanda, M., Abdullah, F., 2019, Fault Mapping in Weh Island based on Fault Fracture Density Method (FFD), *Journal of Aceh Physics Society*, 8, , 2355-8229.
24. Febga, J., Zidan, M., Wangi, GP, and Arifin, ETN 2022. Detection of Geothermal Manifestations Using Landsat 8 Imagery (Case Study of the Mount Patuha Area. *Geographic Information Science. Indonesian Education University. Jurnal Swarnabhumi*, Vol .7, No. 2.
25. Mirwanda, S., Salsabila, F., Pramesti, R., Zakiyyah, A. R., dan Tuelzar, M. R. 2021. Pemetaan Suhu Permukaan Anomali Panas Bumi Daerah Gunung Ciremai Menggunakan Data Inframerah Termal Landsat 8. *Jurnal Geosains Dan Remote Sensing*, 2(2), 92-99.
26. Cahyono, BE, Jannah, N., and Suprianto, A. 2019. Analysis of the Distribution of Geothermal Potential and Manifestations of the Ijen Mountains Based on Surface Temperature and Geomorphology. *Natural B. Vol. 5.No. 1*.
27. Zhang, N., Qin., He, L., and Jiang, H. 2012. Remote Sensing and GIS Based Geothermal Exploration in Southwest Tengchong, China. *Geoscience and Remote Sensing Symposium (IGARSS), IEEE International*, 5364-5367.
28. Williams, R. S. 1983. “Geological Applications”, In. Colwell, R.N. (eds). “Manual of Remote Sensing”, 1667- 1951. Falls Church, VA: American Society of Photogrammetry.
29. Maharani, A., Salsanur, V., Hilal, A., and Aprilian, Y. 2021. Preliminary Interpretation for Geothermal Potential Area Using DEM And Landsat OLI 8 in Mount Endut . *Bulletin of Scientific Contributions: Geology*, 19(1), 35-46.
30. Saraswati, GP, Prasetyo, Y., Sukmono, A. 2019. Analysis of Geothermal Energy Estimates and Recommendations for Geothermal Power Plant Locations Using Landsat 8 Imagery (Case Study: Ungaran Mountain Area, Central Java): *UNDIP Geodesy Journal Vol. 8, no. 1*.

How to cite this article: Alma Izzatinavia, Tony Yulianto, M. Irham Nurwidyanto. Geothermal prospect zone estimation based on Landsat 8 satellite imagery (case study around Gedongsongo). *International Journal of Research and Review*. 2024; 11(6): 68-78. DOI: <https://doi.org/10.52403/ijrr.20240609>
